

Fabrication of photocatalytic PVA–TiO₂ nano-fibrous hybrid membrane using the electro-spinning method

Nguyen Thuy Ba Linh · Kap-Ho Lee ·
Byong-Taek Lee

Received: 28 January 2011 / Accepted: 25 March 2011 / Published online: 7 April 2011
© Springer Science+Business Media, LLC 2011

Abstract Nano-fiber membranes hold great promise for use in filtration applications. In this study, a photocatalytic polyvinyl alcohol (PVA)/TiO₂ composite polymer membrane was successfully synthesized at different TiO₂ concentrations (20, 30, 40, and 50%) using the electro-spinning method. The parameters of electro-spinning including electrical field, tip-to-collector distance, and feed rate were optimized for fabrication process. The diameter of the electro-spun PVA–TiO₂ fibers and average size of the TiO₂ nano-particles loaded in the PVA nano-fibers ranged from 100 to 150 nm and 15 to 30 nm, respectively. X-ray diffraction analysis indicated that the main crystal structure was of the anatase type even though small rutile peaks were also observed for the PVA–TiO₂ membrane. TiO₂ nano-particles were embedded in the PVA fiber and were dispersed linearly along the fiber direction. As the amount of TiO₂ loaded in PVA increased, the tensile strength also increased while the tensile strain significantly decreased. Also, when the TiO₂ content was increased from 20 to 50%, the photocatalytic activity of the PVA–TiO₂ membranes increased.

Introduction

Nano-fibrous media has recently received significant attention due to its low basis weight, high permeability, and small pore size, all of which make this material appropriate for a wide range of filtration applications. In addition, nano-fiber membrane offers unique properties like high specific surface area, good interconnectivity of pores, and potential to incorporate active chemistry or functionality on the nano-scale [1]. Therefore, nano-fibrous media have been extensively studied in the context of air and liquid filtration applications. Nano-fibrous filtering media can be used where high-performance air purification is needed such as in hospitals, healthcare facilities, research labs, and electronic component manufacturers [1–5]. The nano-fiber-based filtering media, which is made up of fibers with diameters ranging from sub-microns to a few nanometers, can be conveniently produced using the electro-spinning technique [6, 7]. This technique has received a lot of attention in recent years because of the relative simplicity with which a wide range of porous structures can be produced and advances in the electro-spinning method has allowed for the industrial production of more than 20 types of fiber filter materials [1, 2, 8–13]. Therefore, the electro-spinning method is suitable for the fabrication of filter media [1, 10, 14] for biomedical applications [15], including tissue engineering of scaffolds [16, 17] and drug delivery [18].

TiO₂ was selected as our target because of its important role in environmental cleaning and protection due to its ability to photocatalyze [19, 20] and decompose harmful organic compounds and low cost [11, 21–25]. TiO₂ is usually used as a powder in solution, which has high photocatalytic efficiency [26]. However, the catalysts should be separated from the purified water after treatment.

N. T. B. Linh · B.-T. Lee (✉)
Department of Biomedical Eng. & Mater., School of Medicine,
Soonchunhyang University, 366-1 Ssangyong dong,
Cheonan 330-090, South Korea
e-mail: lbt@sch.ac.kr

K.-H. Lee
School of Advanced Materials Engineering, Chungnam National
University, Yuseong-gu, Daejeon 305, South Korea

To solve this problem, a photocatalytic membrane reactor has been developed using various membrane techniques [27–29]. In regards to commercial air filtration applications, polymeric nano-fibers has several potential advantages due to the submicron fibers size, which is known to provide better filter efficiency [9, 13]. Among the polymeric nano-fibers, polyvinyl alcohol (PVA) has extensive applications in air filtration, textile industry, and paper coating due to its flexibility and good chemical and thermal stability [3, 4, 10, 11, 30]. In addition, the PVA membrane has higher filtration efficiency because of its nano-fiber diameter [10].

The main purpose of this study was to fabricate a hybrid photocatalytic PVA/TiO₂ membrane that could be used in filtration applications. PVA–TiO₂ nano-fiber membranes were prepared by electro-spinning at the various TiO₂ concentrations (20, 30, 40, and 50%). In addition, the optimized electro-spinning conditions for fabrication of the PVA–TiO₂ membrane were investigated. The crystal structure of the membranes was determined using X-ray diffraction (XRD) and high resolution transmission electron microscopy (HRTEM). Also, the tensile strength and photocatalytic activity of the membranes were investigated as a function of TiO₂ concentration.

Materials and methods

Materials and electro-spinning setting

99+ % hydrolyzed poly (vinyl alcohol), PVA, with a number average Mw of 115,000 g/mol was obtained from Aldrich Chemical Co (USA). TiO₂ nano-particles were prepared using the sol–gel process [31]. The surface area of nano-scale primary particles of TiO₂ (ranging from 15 to 30 nm in diameter) was assessed by BET and found to be 46.52 m²/g. TiO₂ nano-particles contained both rutile and anatase crystals.

Aqueous PVA solutions (12 wt%) were prepared by dissolving in deionized (DI) water at 80 °C with constant stirring for at least 3 h. TiO₂ nano-particles at the following compositions; (w/w between TiO₂ and PVA concentration in DI) 20% (PVA–20TiO₂), 30% (PVA–30TiO₂), 40% (PVA–40TiO₂), and 50% (PVA–50TiO₂) were dispersed in DI water for 1 h and then poured into a PVA solution to obtain a PVA–TiO₂ solution.

The electro-spinning (eS-robot, Electro-spinning/Spray system) solutions were placed into a 10 mL syringe fitted to a needle with a tip diameter of 25 gauges (inner diameter 0.25 mm). A syringe pump (lure-lock type, Korea) was used to control the feed rates, and a grounded cylindrical stainless steel mandrel was used to collect the mat. The electro-spinning voltage was supplied directly by a high

DC voltage power supply (NNC–30 kilovolts—2 mA portable type, Korea).

Characterization of PVA–TiO₂ membranes

The morphologies of the electro-spun PVA fibers and PVA–TiO₂ fibers were examined by scanning electron microscopy (SEM, JSM-7401F), energy dispersive spectrometer (EDS, JSM-7401F), and transmission electron microscopy (TEM) (JEM2010, JEOL, Japan). A small section of the fiber mat was placed on the SEM sample holder and sputter coated with platinum (Cressington 108 Auto). An accelerating voltage of 15 kV was used to take the SEM images. The crystal structures of the PVA–TiO₂ composite polymer membranes were subjected to XRD (Rigaku, D/MAX—2500 V) using Cu K α radiation generated at 40 kV and 200 mA. The diffraction angle was varied from 10 to 80° 2 θ .

The tensile strength of the electro-spun fibrous membranes was determined using an universal testing machine (R&B UNITECH—T, Korea). All samples were prepared in the form of a rectangular shape with a width x length dimension of 4 × 20 mm from the electro-spun fibrous membranes. The thicknesses of the samples were measured using a digital micrometer that had a precision of 1 μ m. The measurements were taken with a 500 g/f load cell. Load–deformation data were recorded at a deforming speed of 0.5 mm/s, and the stress–strain curve of the nano-fibrous structure was constructed from the load–deformation curve.

Photocatalytic performance and characterization of PVA–TiO₂ nano-fiber

The photocatalytic activity of PVA–TiO₂ was investigated by measuring the decomposition of methyl orange (MO), which is a target pollutant. PVA–TiO₂ membranes were placed in DI-containing MO solution (10 mg/L) in Pyrex beakers. A 40 W medium-pressure mercury lamp, which emitted light in the wavelength range of 250–390 nm, was used as the UV irradiation source. A small amount of the solution taken from the reaction solution were analyzed by an UV–Visible spectrometer (HP8453, Hewlett Packard, USA) to determine the residual concentration change of MO during UV irradiation. The absorption of MO was measured in the range from 300 to 700 nm.

Results and discussion

The electro-spinning conditions were optimized to produce a thinner and more uniform PVA–TiO₂ nano-fiber. The optimized conditions were determined by examining the

effect of different electro-spinning parameters, including the PVA–TiO₂ ratio, the applied voltage, tip-to-collection distance (TCD) and feed rate, on the resulting PVA–TiO₂ nano-fibers. The conditions tested are shown in Table 1. First, we fixed the TCD at 10 cm. Then, the applied voltage was varied between 22 and 25 kV. The solution flow rate was also varied between 0.1 and 0.5 mL/h using a syringe pump. Based on these results, the following electro-spinning conditions were shown to result in the formation of thinner and regular PVA–TiO₂ fibers: concentration—PVA, 12 wt%; TCD, 10 cm, voltage, 25 kV, and flow rate, 0.1 mL/h.

Figure 1 shows the effect of the TiO₂ content on the morphology of fibers. The appearance of TiO₂ nano-particles in PVA fibers clearly increased when increasing the concentration of TiO₂. TiO₂ nano-particles were well distributed in the PVA nano-fibrous matrix. The reasons no coagulation of the TiO₂ nano-particles were observed in the matrix was most likely due to the interaction between the PVA solution and TiO₂ nano-particles and the strong electric field during electro-spinning. The interaction caused by hydrogen bonding between hydroxide groups in PVA and oxygen in TiO₂ may have prevented TiO₂ nanoparticle aggregation. The average diameter of the PVA–TiO₂ fibers was determined from SEM and is shown in Table 1. The diameter of the electro-spun PVA–TiO₂ fibers was found to decrease from 150 to 100 nm as the content of TiO₂ increased from 20 to 50%.

Figure 2 showed a high magnification SEM image and EDS profile of PVA-50% TiO₂. TiO₂ nano-particles were loaded on the surface of PVA fibers and were dispersed linearly along the fiber direction, which originated from the effect of polarization and orientation caused by the high electric field during electro-spinning method. The EDS profile in Fig. 2b shows that the TiO₂ nano-particles were successfully loaded into the PVA nano-fibers.

The XRD measurements were performed to examine the crystalline structure of the PVA–TiO₂ composite polymer membrane. Figure 3 shows the XRD patterns of the PVA–TiO₂ composite at different TiO₂ concentrations. PVA nano-fibers of higher molecular weight had a superior

crystalline property with a prominent peak around 19° 2θ. As can be clearly seen in Fig. 3, TiO₂ in all of the PVA–TiO₂ composite polymer membranes had both an anatase and rutile structure. The strong peaks of anatase at 25.2°, 37.8°, 48.0°, 53.9°, 62.7°, and the few peaks of rutile are clearly observed in Fig. 3. This result confirmed that TiO₂ nano-particles loaded in the PVA nano-fibers retained their crystalline structure even in the high electrostatic field used during electro-spinning.

The TEM and HRTEM were used to image the internal microstructure of the electro-spun PVA–50TiO₂ composite membrane. As shown in Fig. 4a, the diameter of the PVA–50TiO₂ fiber was approximately 100 nm, and TiO₂ nano-particles were well dispersed throughout the surface of the PVA nano-fiber. The electron diffraction pattern, which was taken from the center of the PVA nano-fibers, confirmed that the TiO₂ nano-particles were dispersed with a random orientation. From the HRTEM analysis (Fig. 4b), lattice TiO₂ nano-particles with a highly crystalline structure and diameter of approximately 15 nm were clearly observed. When the solution was ejected from the nozzle, which was connected to the positive electrode of the high-voltage power supply, the jet took a positive charge and both the surface of the fibers and TiO₂ nano-particles within the fibers became positively charged. Consequently, the positively charged TiO₂ nano-particles were repulsed by the positive charges on the surface of the fibers and aggregated in the middle of the fibers. Furthermore, the high electric field induced the polarization and orientation of the TiO₂ nano-particles; thus, the TiO₂ nano-particles became embedded in and aligned along the direction of the fiber.

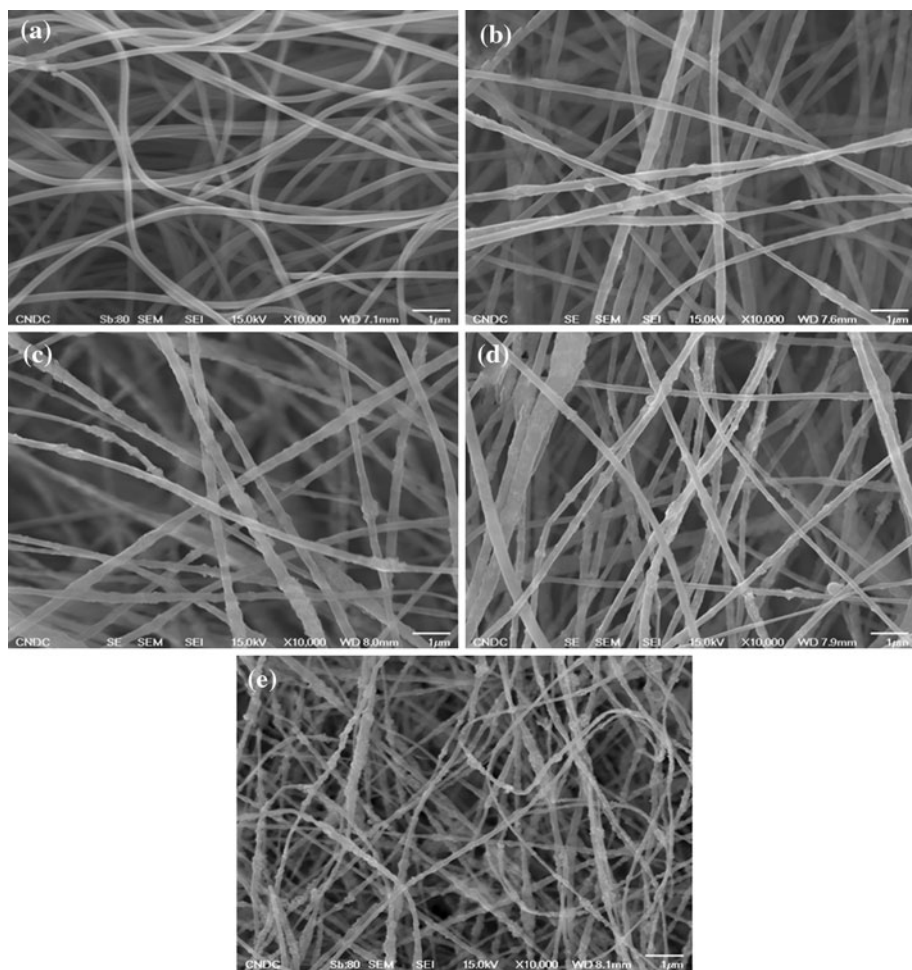
The stress-strain curves of the electro-spun fibrous membranes of PVA–TiO₂ at different TiO₂ concentrations are shown in Fig. 5, and the tensile strength and strain are listed in Table 2. The tensile strength of the PVA–TiO₂ increased from 1.65 to 4.15 MPa as the concentration of TiO₂ increased from 20 to 50%, respectively. This result implies that the dispersion strengthening effect occurred due to the dispersion of nano-sized TiO₂ particles. When

Table 1 Electrospinning conditions used for the fabrication of PVA–TiO₂ membranes at different TiO₂ concentrations

Samples	Average diameter of fibers ^a (nm)	Parameter		
		Voltage (kV)	Distance (cm)	Feed rate (mL/h)
PVA	150 ± 20	22	10	0.5
PVA–20TiO ₂	150 ± 20	22	10	0.5
PVA–30TiO ₂	150 ± 20	22	10	0.5
PVA–30TiO ₂	120 ± 20	25	10	0.5
PVA–40TiO ₂	120 ± 20	25	10	0.5
PVA–40TiO ₂	100 ± 20	25	10	0.1
PVA–50TiO ₂	100 ± 20	25	10	0.1
PVA–50TiO ₂	100 ± 20	25	10	0.5

^a All data are expressed as mean ± standard deviation

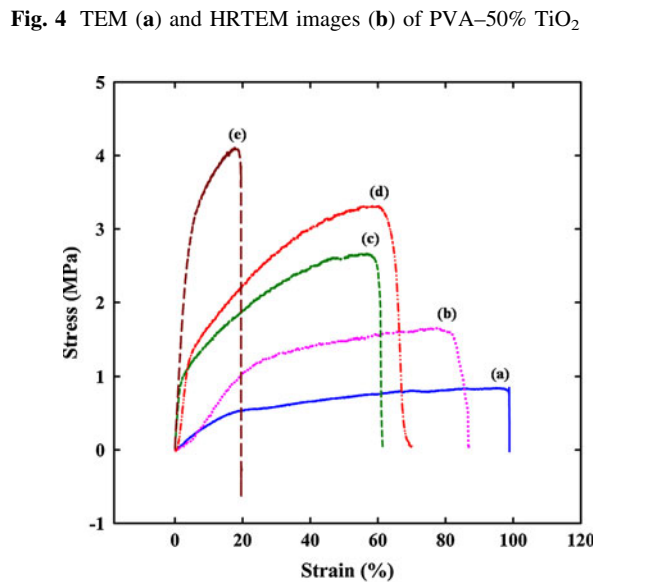
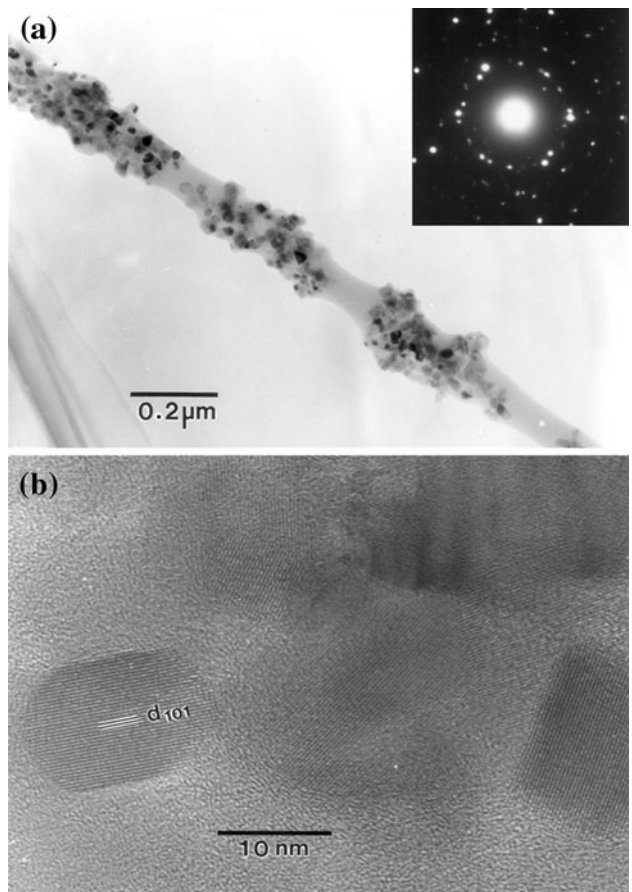
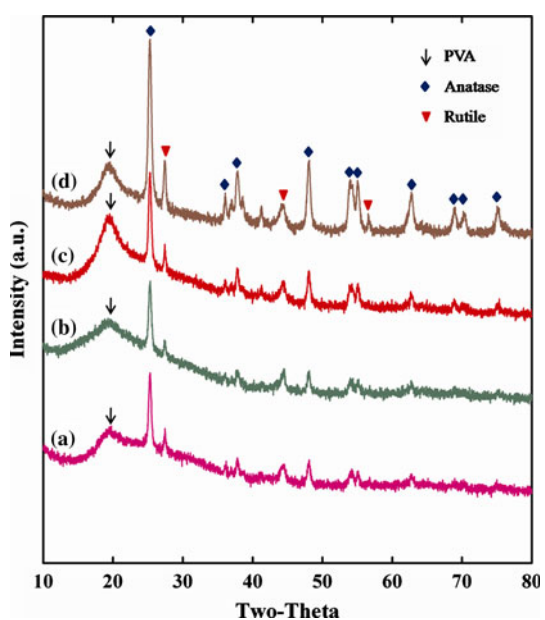
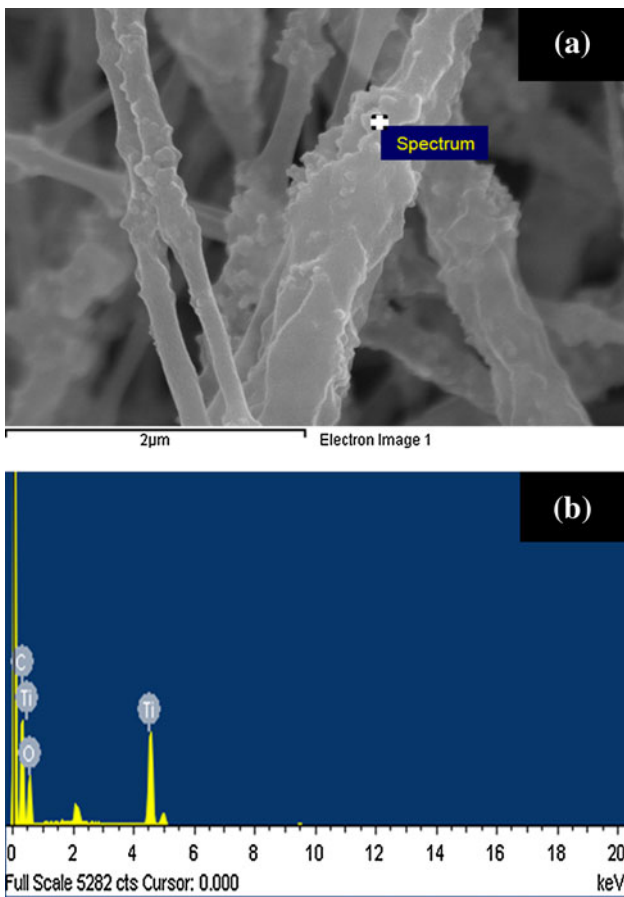
Fig. 1 SEM images of **a** PVA and PVA–TiO₂ at different TiO₂ concentrations; **b** 20%, **c** 30%, **d** 40%, and **e** 50%



the TiO₂ concentration was increased, the tensile strength increased while the strain decreased. The effect of the TiO₂ nano-particle concentration on mechanical behavior can be explained by the interfacial adhesion between the TiO₂ nano-particles and PVA. In addition, as the TiO₂ nano-particle contents increased, the strain at failure of the composites tended to decrease because of a decrease in flexibility. This result implies that the loading of TiO₂ can improve the tensile strength of PVA membranes.

The MO was used to test the photocatalytic activity of the PVA–TiO₂ membrane. The concentration of the MO solution was measured as a function of UV irradiation time using UV–Vis spectrophotometer. The changes in concentration of the MO solutions were evaluated based on the changes in absorbance. The photocatalytic degradation of MO on PVA–TiO₂ till 900 min is shown in Fig. 6. At the first 90 min, all of the membranes showed a rapid activity in degrading MO under UV irradiation. After this stage a relatively slower activity was recorded. After 240 min of UV irradiation, a significant amount of entire MO had been decomposed on the PVA–50TiO₂ membrane. But for complete degradation of MO, it took almost 540 min in

case of PVA–50TiO₂. This was in fact a quick and efficient filter activity compared with others. For example, PVA–20TiO₂, PVA–30TiO₂, and PVA–40TiO₂ showed a slower activity than PVA–50TiO₂ to degrade MO under UV exposure (Fig. 6). The photocatalytic degradation of the organic dye was initiated by photoexcitation of the semiconductor, followed by the formation of an electron–hole pair on the surface of the catalyst. The high oxidation hole directly oxidized the dye resulting in its degradation. Very reactive hydroxyl radicals can also be formed either by the decomposition of H₂O or by the reaction of the hole with OH[−]. The hydroxyl radicals can also easily degrade the organic dye [27]. The rate of MO decomposition increased as the concentration of TiO₂ increased. The removal efficiencies of organic pollutants should significantly decrease when the photocatalytic active surface area is decreased. The surface area of fibers is directly influenced by the fiber diameter. As the fiber diameter narrows, the surface area increases. However, the fiber diameter of materials is dictated by PVA–TiO₂ composition. From Fig. 1, it is found that PVA–50TiO₂ fibers are smaller than that of the other concentrations used here along with TiO₂, which can be



interpreted that that PVA–50TiO₂ had a higher surface area than the others. Therefore, high concentration of TiO₂ in the nano-fiber membranes resulted in a high active surface

Table 2 Tensile strength of PVA–TiO₂ at different TiO₂ concentrations

Samples	Ultimate strength ^a (MPa)	Strain ^{a,b} (%)
PVA–20TiO ₂	1.65 ± 0.40	81.5 ± 5.0
PVA–30TiO ₂	2.71 ± 0.50	58.0 ± 5.0
PVA–40TiO ₂	3.33 ± 0.50	60 ± 5.0
PVA–50TiO ₂	4.15 ± 0.50	19 ± 5.0

^a All data are expressed as mean ± standard deviation

^b At ultimate strength

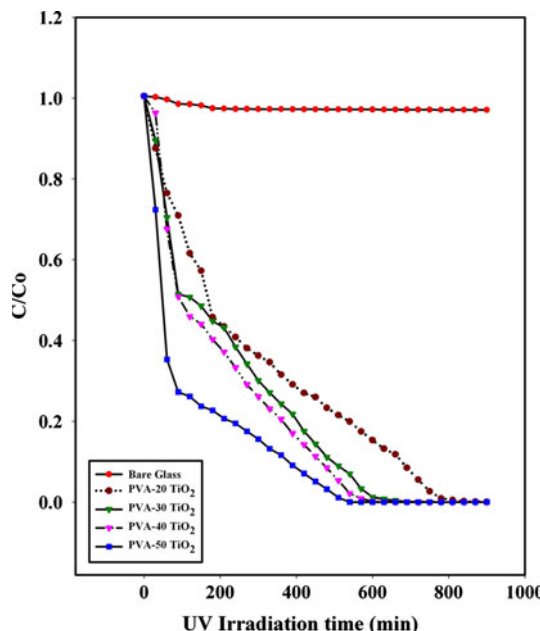


Fig. 6 The photocatalytic degradation of MO on PVA–TiO₂ at different TiO₂ concentrations after 4 h under UV irradiation

area which actually enhanced the photocatalytic activity. Thus, the PVA–50TiO₂ membrane exhibited the best photocatalytic performance.

Conclusions

PVA–TiO₂ composite polymer membranes for filtration applications were prepared successfully using the electro-spinning method. The optimal electro-spinning conditions for the fabrication of PVA–TiO₂ membranes, such as the concentration of TiO₂ nano-particles, voltage, and flow rate, were determined and under these optimized conditions nano-scale structures were obtained (100–150 nm). TiO₂ nano-particles were well dispersed on the surface and inside of the PVA nano-fibers. TiO₂ nano-particles with a crystalline structure can improve the tensile strength of

PVA–TiO₂ membranes. The PVA–50TiO₂ membrane exhibited good photocatalytic performance in regards to the degradation of methyl orange. A hybrid electro-spun PVA–TiO₂ membrane with efficient photocatalytic activity was fabricated and demonstrated to be a highly promising candidate for use in filtration applications.

References

- Barhate RS, Ramakrishna S (2007) J Membr Sci 296:1
- Byoung Chan K et al (2005) Nanotechnology 16:S382
- Jonggeon J, Lee KH (1999) J Appl Polym Sci 72:1755
- Qin XH, Wang SY (2008) J Appl Polym Sci 109:951
- Ye P, Xu ZK, Wu J, Innocent C, Seta P (2005) Macromolecules 39:1041
- Greiner A, Wendorff JH (2007) Angew Chem Int Ed 46:5670
- Ramakrishna S, Jose R, Archana PS, Nair AS, Balamurugan R, Venugopal J, Teo WE (2010) J Mater Sci 45(23):6283. doi: [10.1007/s10853-010-4509-1](https://doi.org/10.1007/s10853-010-4509-1)
- Eda G, Shivkumar S (2006) J Mater Sci 41:5704. doi: [10.1007/s10853-006-0069-9](https://doi.org/10.1007/s10853-006-0069-9)
- Kong C, Lee T, Lee S, Kim H (2007) J Mater Sci 42:8106. doi: [10.1007/s10853-007-1734-3](https://doi.org/10.1007/s10853-007-1734-3)
- Gopal R, Kaur S, Ma Z, Chan C, Ramakrishna S, Matsuura T (2006) J Membr Sci 281:581
- Wang H, Zheng G, Sun DH (2007) In: Proceedings of the 7th IEEE, international conference on nanotechnology, Hong Kong, August 2–5
- Qin XH, Wang SY (2006) J Appl Polym Sci 102:1285
- Zhang L, Menkhaus TJ, Fong H (2008) J Membr Sci 319:176
- Brown RC (1993) Air filtration. Pergamon Press, Oxford
- Agarwal S, Wendorff JH, Greiner A (2008) Polymer 49:5603
- Nguyen TH, Lee BT (2010) J Mater Sci Mater M 21:1969
- Nguyen TH, Lee KH, Lee BT (2010) Mat Sci Eng C Bio S 30:944
- Sill TJ, von Recum HA (2008) Biomaterials 29:1989
- Kanjwal Muzafar A, Barakat Nasser AM, Sheikh Faheem A, Kim HY (2010) J Mater Sci 45(5):1272. doi: [10.1007/s10853-009-4078-3](https://doi.org/10.1007/s10853-009-4078-3)
- Chandrasekar R, Zhang L, Howe JY, Hedin NE, Zhang Y, Fong H (2009) J Mater Sci 44(5):1198. doi: [10.1007/s10853-008-3201-1](https://doi.org/10.1007/s10853-008-3201-1)
- Hoffmann MR, Martin ST, Choi W, Bahnemann DW (1995) Chem Rev 95:69
- Lin J, Yu JC (1998) J Photochem Photobiol A Chem 116:63
- Wold A (1993) Chem Mater 5:280
- Yamaguchi K, Inumaru K, Oumi Y, Sano T, Yamanaka S (2009) Microporous Mesoporous Mater 117:350
- Zhong JB, Lu Y, Jiang WD, Meng QM, He XY, Li JZ, Chen YQ (2009) J Hazard Mater 168:1632
- Luo Q, Li X, Wang D, Wang Y, An J (2011) J Mater Sci 46:1646. doi: [10.1007/s10853-010-4981-7](https://doi.org/10.1007/s10853-010-4981-7)
- Doh SJ, Kim C, Lee SG, Lee SJ, Kim H (2008) J Hazard Mater 154:118
- Molinari R, Borgese M, Drioli E, Palmisano L, Schiavello M (2002) Catal Today 75:77
- Molinari R, Palmisano L, Drioli E, Schiavello M (2002) J Membr Sci 206:399
- He CH, Gong J (2003) Polym Degrad Stab 81:117
- Lee BT, Han JK, Gain AK, Lee KH, Saito F (2006) Mater Lett 60:2101